Contents lists available at SCCE

Journal of Soft Computing in Civil Engineering

Journal homepage: www.jsoftcivil.com

Attenuation Models for Estimation of Vertical Peak Ground Acceleration Based on PSO Algorithm for the North of Iran

Elham Mohammad Kamareh[1], Javad Mokari Rahmdel[2], Akbar Shirzad[3*], Rashed Poormirzae[4]

1. M.Sc. Student in Civil-Earthquake Engineering, Faculty of Civil Engineering, Urmia University of Technology, Urmia, Iran
2. Assistant Professor, Faculty of Civil Engineering, Urmia University of Technology, Urmia, Iran
3. Associate Professor, Faculty of Civil Engineering, Urmia University of Technology, Urmia, Iran
4. Assistant Professor, Faculty of Mining Engineering, Urmia University of Technology, Urmia, Iran

Corresponding author: *a.shirzad@uut.ac.ir*

https://doi.org/10.22115/SCCE.2023.374235.1576

ARTICLE INFO

Article history:
Received: 02 December 2022
Revised: 14 February 2023
Accepted: 04 April 2023

Keywords:
Attenuation relationships;
Northern Iranian plateau;
Optimization;
PSO algorithm;
Vertical PGA component.

ABSTRACT

Peak ground acceleration (PGA) is a critical parameter in ground-motion investigations, in particular in earthquake-prone areas such as Iran. In the current study, a new method based on particle swarm optimization (PSO) is developed to obtain an efficient attenuation relationship for the vertical PGA component within the northern Iranian plateau. The main purpose of this study is to propose suitable attenuation relationships for calculating the PGA for the Alborz, Tabriz and Kopet Dag faults in the vertical direction. To this aim, the available catalogs of the study area are investigated, and finally about 240 earthquake records (with a moment magnitude of 4.1 to 6.4) are chosen to develop the model. Afterward, the PSO algorithm is used to estimate model parameters, i.e., unknown coefficients of the model (attenuation relationship). Different statistical criteria showed the acceptable performance of the proposed relationships in the estimation of vertical PGA components in comparison to the previously developed relationships for the northern plateau of Iran. Developed attenuation relationships in the current study are independent of shear wave velocity. This issue is the advantage of proposed relationships for utilizing in the situations where there are not sufficient shear wave velocity data.

How to cite this article: Mohammad Kamareh E, Mokari Rahmdel J, Shirzad A, Poormirzae R. Attenuation models for estimation of vertical peak ground acceleration based on PSO algorithm for the north of Iran. J Soft Comput Civ Eng 2023;7(3):129–142. https://doi.org/10.22115/scce.2023.374235.1576

1. Introduction

Several major earthquakes have been occurred in Iranian Plateau that some of them are shown in Table 1. Attenuation relationships have an integral role in the analysis of seismic risk [1]. These relationships are commonly used to estimate the uncertainty in earthquake motion in conventional hazard analysis [2]. Major earthquakes in Kobe (1995), Bam (2003) and Chi Chi (1999) have highlighted the importance of the vertical component of the earthquake in the extent of damage to diverse building systems [3,4]. Numerous studies have been conducted on the importance of the vertical component of earthquake that are mentioned in the following.

Table 1
Some major earthquakes in Iran.

Location (Province)	Year	Damage (death toll)	Local magnitude
Sarpol-e Zahab (Kermanshah)	2018	over 500 wounded	6.35
Ahar-Varzaghan (East Azarbaijan)	2012	306 killed & 3037 wounded	6.35
Mormori(Ilam)	2014	over 250 wounded	6.17
Taze abad (Kermanshah)	2014	3 killed & 243 wounded	6.17
Sang Chal (Mazandaran)	1957	1500 killed	6.74
Buin Zahra (Qazvin)	1962	over 12225 killed & 2800 wounded	6.82
Dasht-e Bayaz (Sothern Khorasan)	1968	about 10000 killed	6.8
Korizan Khaf (Khorasan)	1979	420 killed	6.19
North east of Kish island (Hormozgan)	2022	1 killed & 30 wounded	5.7
Bakhtar Sarjangal (Sistan and Baluchestan)	2022	0	5.6

Terzi and Athanatopoulou (2021), by studying a historical building in Greece, concluded that the role of the vertical component on the total number of effective building cracks is significant [5]. Rahai and Arezoumandi (2008) analyzed a reinforced concrete bridge pier and they showed that vertical movements during the earthquake increased the response level and extent of the damage to the bridge [6]. They also found that vertical movements result in axial forces acting on the bridge columns which in turn, cause instability of hysteresis loops and increase the extent of damage. Consequently, in addition to the horizontal component of earthquake, the effects of the vertical component of the earthquakes should also be considered in the seismic design of structures. Vertical accelerations can change gravity loads that control the in-plane lateral load capacity of masonry foundations and affect the out of plane overturning stability of thin-walled panels [7]. Noteworthy, higher acceptable performance levels of the steel beams (larger plastic rotations) occur when both horizontal and vertical seismic components are considered [8]. The majority of researchers believe that it is important to consider the effect of the vertical component in high-rise structures and those constructed near faults [9].

So far, many efforts have been made by researchers to analyze seismic risk by looking for a suitable attenuation relationship between effective parameters of PGA such as magnitude, distance, fault depth and geotechnical conditions. Statistical modeling such as regression analysis is commonly used to estimate the relationship between two or more variables [10]. Many scholars such as Zaré (1999), Ambraseys et al. (2005), Sedaghati and Pezeshk (2017), Soghrat and Ziyaeifar (2017) and Ghodrati Amiri et al. (2018) used a variety of regression methods for the estimation of PGA [4,11–14]. In addition, optimization techniques such as the genetic

algorithm (GA) have also been used in the last decades to solve a wide variety of optimization problems such as structural damage detection optimization [15–17]. Amit Shiuly et al. (2020) used the genetic algorithm and an artificial neural network model to predict the PGA of Himalayan region in India [18]. They used the hypocenter distance and magnitude as input parameters and PGA records at different distances as output parameters. They compared their results to the result of other attenuation relationships and concluded that GA and ANN algorithms are capable to predict PGA values.

Sobhaninejad et al. (2007) used the GA with 586 data records from Europe and the Middle East to modify the attenuation relationships proposed by Ambraseys et al. (2005) [12,19]. Also, Bagheri et al. (2011) used the GA in Alborz, Central Iran and Zagros then proposed new relationships to estimate PGA and peak spectral acceleration (PSA) [15]. Regarding the lack of attenuation relationships in the vertical direction in the northern Iran plateau, the aim of this study is to extract attenuation relationships in the vertical direction using the particle swarm optimization (PSO) algorithm. To this aim, firstly, about 270 earthquake records are used to extract the initial model (an explicit equation between PGA and involved parameters), and then the PSO algorithm is applied to find the proper coefficients to predict the adequate PGA values for northern part of Iran. Finally, the results of developed attenuation relationships in this paper are compared to previously developed ones.

2. Research significance

In the present research it is tried to develop attenuation models for estimation of vertical PGA based on the PSO algorithm for the North of Iran. The importance of using such attenuation relationships, is in the seismic design of more resistant buildings and preventing more damage to buildings.

3. Methods

3.1. Particle swarm optimization (PSO) algorithm

The PSO algorithm was proposed by Eberhart and Kennedy (1995), which was inspired from the food searching behavior of birds (called particles) swarms [20]. The PSO algorithm is a subset of the swarm-based algorithms, and swarm-based algorithms are a subclass of nature-inspired algorithms, and nature-inspired algorithms are a subset of meta-heuristic algorithms. Meta-heuristic algorithms use intelligent strategies to explore a wide search space efficiently. These algorithms, in contrast to deterministic algorithms, e.g., the simplex method, because of their intelligent searching mechanisms are capable of finding global optimum effectively. In the last decades, swarm-based algorithms, especially PSO algorithm, have been widely used in different engineering problems [21–24]. The PSO algorithm in comparison to other well-known algorithms such as the genetic algorithm (GA) is simpler and easier to apply. Different comparative studies showed that the PSO algorithm was superior to other meta-heuristic algorithms in finding the final optimum solution/model [25,26]. In the PSO algorithm, individuals (birds or particles) in an n-dimensional search space are considered potential solutions. The initial swarm/population for each variable in the determined range is randomly

generated. In an iterative procedure and by fitness function (error function) the particles are evaluated and then the best particle (a particle with the lowest value of error) is introduced (called g_{best}). In addition, each particle keeps its best position (position with the lowest value of error) (called p_{best}) that has been visited by the particle so far. In the PSO algorithm, the velocity of each particle that moves towards p_{best} and also g_{best} changes frequently. If the k[th] particle in an n-dimensional space is considered to be $x^k = \mathrm{x}_1^k, \mathrm{x}_2^k, \dots, \mathrm{x}_n^k$, the p_{best} of this particle will be presented by $(\mathrm{p}_{best})_k = (\mathrm{p}_{best})_{k.1}, (\mathrm{p}_{best})_{k.2}, \dots, (\mathrm{p}_{best})_{k.n}$. The best particle among all particles is represented by $g_{best} = g_{best.1}, g_{best.2}, \dots, g_{best.n}$ [27]. The velocity of the kth particle is shown by $\mathrm{v}^k = \mathrm{v}^{k.1}, \mathrm{v}^{k.2}, \dots, \mathrm{v}^{k.n}$. The velocity and position of the particles are set using the following equations:

$$\mathrm{v}_{t+1}^k = w\mathrm{v}_t^k + c_1 rand_1.\left((\mathrm{p}_{best})_k - x_t^k\right) + c_2 rand_2.\left(g_{best} - x_t^k\right) \quad (1)$$

$$\mathrm{x}_{t+1}^k = \mathrm{x}_t^k + \mathrm{v}_{t+1}^k \qquad , \mathrm{k} = 1,2, \dots, \mathrm{pop} \quad (2)$$

where *pop* and *t*, respectively, indicate the number of particles and iterations, v_t^k and v_{t+1}^k denote the velocity of the k^{th} particle in the t^{th} and $(t+1)^{th}$ iterations, respectively. Also, *w* represents the inertia weight coefficient, c_1 and c_2, respectively, show acceleration factors that pull the particle towards its p_{best} and g_{best}. Moreover, $rand_1$ and $rand_2$, respectively, represent uniform random numbers in the range of [0, 1] and x_t^k and x_{t+1}^k are the position of k^{th} particle in the t and (t+1) iterations, respectively [20,28]. Based on the showed pseudo-code of the PSO algorithm in Figure 1, the coding was carried out in MATLAB software R2015a.

```
Begin
 1: Objective function, F_f(X), X=(X^1, X^2, X^3,... X^k)^T
 2: Initialize each particle's velocity and position randomly, X^k (k=1, 2, 3, …, pop)
 3: Find the p^best and g^best by objective/error function
 4: while t < Max_iteration do  (termination condition)
 5:     for k=1:pop
 6:         Update particle velocity and particle position by Eqs.1 and 2
 7:         Evaluate new solution/location
 8:         Check boundary conditions and evaluate new solution/position
 9:         Update  the p^best and g^best
10:     end for
11: end while
12: Output X* (final solution/model)
End
```

Fig. 1. Pseudo-code of the PSO algorithm.

3.2. Collected data

The selected area in this study was the North Iranian Plateau, including Alborz, Azerbaijan and Kopet Dag regions, which are parts of the active tectonic regions of Iran (Figure 2a). The accelerogram data in the present study were selected from the Building and Housing Research Center (BHRC) of Iran, according to the classification of the Standard 2800 (2014), which is similar to Eurocode 8 (CEN, 2003) [29,30]. Earthquake records were classified based on the shear wave velocity of the soil at a depth of 30 m (V_{s30}), i.e., I: V_{s30} >750; II: 375≤V_{s30}≤750; III:

$175 \leq V_{s30} \leq 375$; IV: $V_{s30} < 175$. Finally, about 240 records with a moment magnitude of 4.1 to 6.4 and epicentral distances less than 400 km (7 to 359 km) were selected for further analysis.

Figures 2b and 2c represent the distribution of accelerogram stations and coordinates of the event epicenter in the study area. Due to availability of the epicentral distance for all selected data in the national accelerogram network, it is used as the distance parameter. About 56.66% of whole data have the magnitude of 6-6.4, 29.16% of whole data have the magnitude of 4-5, and remained data have the magnitude of 5-6. Noteworthy, in the current study, the proposed catalog of Karimiparidari et al. (2014) was used to convert the magnitude data which were not on the moment scale [31].

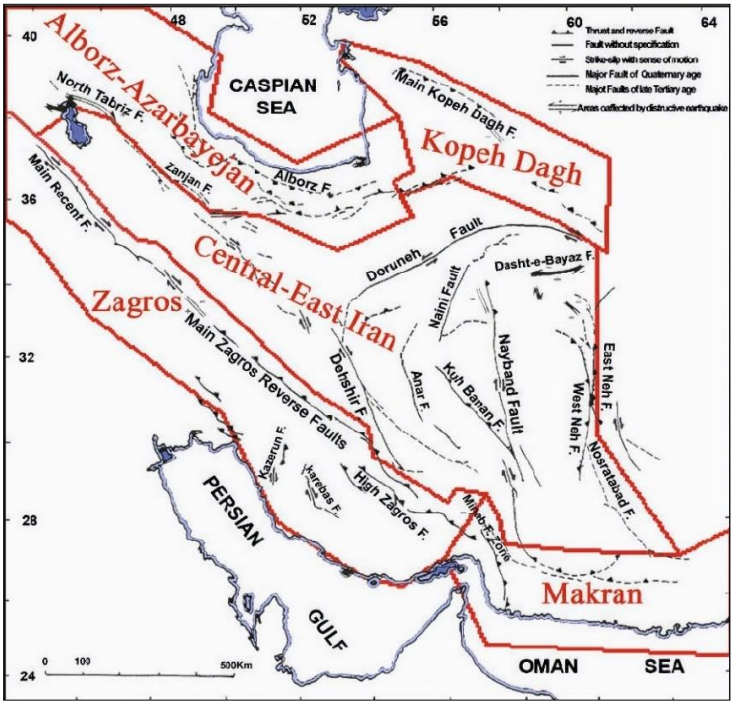

(a) The five active tectonic regions (Mirzaei et al. 1998) [32]

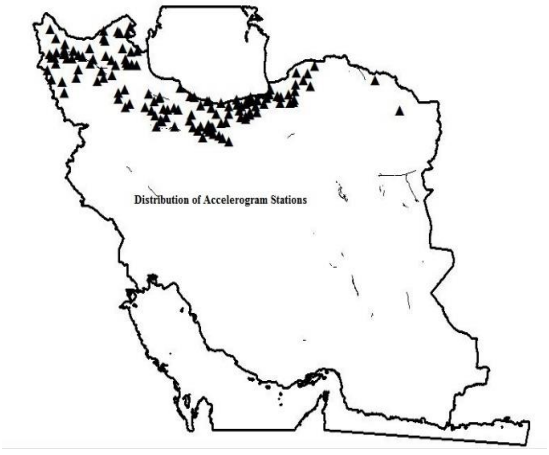

(b) distribution of accelerogram stations

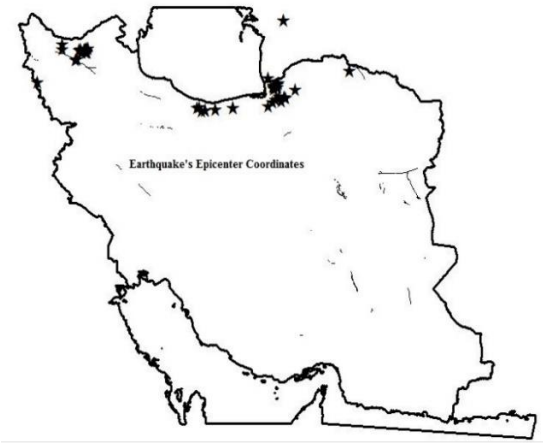

(c) The epicenter coordinates of the selected events

Fig. 2. Location of the studied region, distribution of accelerogram stations and the epicenter coordinates of events.

3.3. Error evaluation criteria

To explore the more efficient models for attenuation relationships, different evaluation criteria such as root mean squared error (RMSE), mean absolute percentage error (MAPE), mean error (ME), coefficient of determination (R^2) and adjusted R^2 ($R^2_{Adjusted}$), are used to assess the results. The RMSE and its combination with MAPE are used as the PSO objective/error function (F_f) for developing attenuation relationships.

Furthermore, the Log-likelihood (LLH) statistical test is used for consistency check between the measured and calculated data [33,34]. The LLH method, in order to compare two models, has widely been used in engineering sciences in the last few years. The value of the LLH criterion changes between 0 and 1, which values toward 1 show the high consistency and vice versa.

3.4. Formulation of optimization objective function

The considered objective functions in the current work, are presented by Eqs. 3 and 4. It should be noted that RMSE minimization was first considered as the objective function (Eq. 3). Regarding the results, the objective function in Eq. 4 was used to improve the optimization results where α and β are factors determined by sensitivity analysis. Also, the PGA prediction equations are proposed after sensitivity analysis of several different functions based on the least squared error rate.

$$\text{Objective Function: Minimize } (\mathrm{F_f}) = \mathrm{RMSE} = \sqrt{\frac{\sum_{i=1}^{n}(\mathrm{PGA_{obs}} - \mathrm{PGA_{cal}})^2}{n}} \tag{3}$$

$$Objective\ Function: Minimize\ (F_f) = (\alpha \times MAPE + \beta \times RMSE) \tag{4}$$

where PGA_{cal} is the peak ground acceleration calculated from the attenuation relationships in Eqs. 5 and 6. Eqs. 5 and 6, respectively, estimate PGAs based on the soil and fault types (strike-slip and thrust-reverse faults).

$$log_{10}^{Y} = a_1 + a_2 \exp(a_3 M_w) + a_4 \exp(a_5 R) + a_6 \exp(a_7 F_{TR}) + a_8 \exp(a_9 F_{SS}) + a_{11}(\frac{\sigma_{V_{s30}}}{\mu_{V_{s30}}})^{a_{10}} \tag{5}$$

$$log_{10}^{Y} = a_1 + a_2 \exp(a_3 M_w) + a_4 \exp(a_5 R) + a_6 \exp(a_7 V_{s30}) \tag{6}$$

where a_1 to a_{11} are decision variables obtained from the PSO model, Y stands for PGA, Mw is the moment magnitude, R represents the epicentral distance (km), $V_{s_{30}}$ shows the shear wave velocity for the top 30 m of soil (m/s), F_{SS} is the strike-slip fault parameter; F_{TR} is the thrust-reverse fault parameter and $\sigma_{V_{s30}}$ and $\mu_{V_{s30}}$, respectively, show the standard deviation and mean of shear wave velocities of different soil groups at a depth of 30 m.

4. Discussion

Sensitivity analysis was performed to determine the PSO parameters. According to the results, the internal parameters of the PSO algorithm, i.e., population size, maximum iteration, acceleration coefficients (c_1 and c_2) and inertia weight coefficient (w) were set equal to 300, 1000, 2 and 1, respectively. In this article, different forms of objective functions and attenuation relationships were tested. Finally, the best results were selected for presentation. The objective

function in Eq. 3 was used to obtain attenuation relationships for PGA_v estimation. The results include the best obtained values and the standard deviation of residuals (Table 2). As seen in Table 2, the accuracy of the attenuation relationships is improved by classifying the soil based on the shear wave velocity. Table 3 presents the values obtained for the decision variables, i.e., the coefficients of attenuation relationships for different soil types with different shear wave velocities.

Table 2
The optimization results for estimating PGA_v in the case of using RMSE as the objective function (Eq. 3)

		The best value obtained for objective function	Performance measures		
			$RMSE_T$ *	$MAPE_T$ **	$\sigma_{residual}$ ***
Soil groups	I	0.114	0.22	79.842%	0.251
	II	0.327			
	III	0.716			
All input data		0.292	0.292	80.256%	0.355

*$RMSE_T$ is the weighted mean of RMSEs obtained for every group
**$MAPE_T$ is the weighted mean of MAPEs obtained for every group
*** $\sigma_{residual}$ is the standard deviation of residuals

Table 3
The optimum values of attenuation relation cofficients for estimating PGA_v in the case of using RMSE as the objective function

		Values of decision variables (coefficients of the attenuation relations)										
		a_1	a_2	a_3	a_4	a_5	a_6	a_7	a_8	a_9	a_{10}	a_{11}
Soil groups	I	0.7438	-7.5173	-0.1525	3.1234	-0.0054	-0.2762	-0.0812	-0.0907	-1.9434	1.6421	-0.9170
	II	-0.5187	-9.0524	-0.333	3.0502	-0.0152	0.2737	-1.7204	0.7468	-4.5034	0.8724	-2.9745
	III	3.2382	-6.6793	-0.2334	1.2775	-0.0118	-3.1572	-3.8436	-2.9659	-5.0928	1.7035	2.4601
All input data		-0.8350	-10.00	-0.4256	2.0401	-0.0137	7.0245	-4.3108	0.2116	0.5903	-0.3303	-4.1501

The general objective function, $\alpha \times MAPE + \beta \times RMSE$ (Eq. 4), was used to improve the accuracy of attenuation relationships for PGA_v estimation. After sensitivity analysis based on the different values of coefficients α and β, the objective functions MAPE+2RMSE and MAPE+3RMSE were, respectively, selected for the Tabriz-Kopeh Dagh and Alborz-Khazar faults. In Table 4 acceptable results are shown. Comparing the results in Table 2 and 4 indicates an improvement of MAPE using the combined objective function. Table 5 lists the values that obtained for the coefficients of the attenuation relationship for different fault types.

Table 4
The optimization results for estimating PGA_v in the case of using RMSE and MAPE as the hybrid objective function (Eq. 4)

		The best value obtained for objective function	Performance measures			
			MAPE	$MAPE_T$ **	*$RMSE_T$	$\sigma_{residual}$ ***
Fault types	Tabriz-Kopeh Dagh	1.003	39.821%	42.682%	0.316	0.288
	Alborz-Khazar	1.718	46.422%			

*$RMSE_T$ is the weighted mean of RMSEs obtained for each group
**$MAPE_T$ is the weighted mean of MAPEs obtained for each group
*** $\sigma_{residual}$ is the standard deviation of residual

Table 5
The optimum values of attenuation relation cofficients for estimating PGA_v in the case of using RMSE and MAPE as the hybrid objective function.

		Values of decision variables (coefficients of the attenuation relations)						
		a_1	a_2	a_3	a_4	a_5	a_6	a_7
Fault Types	Tabriz- Kopeh Dagh	0.19602	-8.7819	-0.2684	2.1508	-0.01614	-4.0111	-9.5617
	Alborz- Khazar	-0.7448	9.9998-	-0.4495	1.4815	-0.01645	2.4233	-3.5297

4.1. Comparing the proposed attenuation relationships with other ones

Derived attenuation relationships in this study were compared with those presented in the literature for the north plateau of Iran. To this aim, five attenuation relationships (Table 6) that have been proposed for Europe-Middle East and Iran (North Iranian Plateau) were selected to compare with the proposed relationship in this study.

Table 6
Candidate attenuation relationships.

Attenuation Models	Abbreviation	Type of Distance	M_w Range
Zaré (1999) [11]	Z-9	Focal	3.2-6.4
Nowroozi (2005) [35]	N-5	Epicentral	5.1-6.4
Ghodrati Amiri et al. (2007) [36]	G-7	Focal	5.1-6.4
Soghrat and Ziyaeifar (2017) [4]	SZ-17	Epicentral	4.1-6.4
Sedaghati and Pezeshk (2017) [13]	SP-17	Boore-Joyner	3.2-6.4

The evaluation indices including R^2, $R^2_{Adjusted}$, ME, RMSE, MAPE and LLH were calculated for different attenuation relationships and the results were presented in Table 7. In this table, PGA_v-1 is the proposed model based on the shear wave velocity and objective function of RMSE for PGA_v and PGA_v-3 is the proposed model based on the fault type and hybrid objective function of MAPE and RMSE for PGA_v. According to the results, PGA_v-1 has a lower RMSE than the other selected relationships. The PGA_v-1 and PGA_v-3 models with a higher R^2 and $R^2_{Adjusted}$ outperformed than other relationships. The PGA_v-3 and SZ-17 models showed lower MAPE values than other ones. However, PGA_v-3 outperformed SZ-17 in terms of other evaluation criteria (Table 7). Based on ME, the PGA_v-3 and PGA_v-1 predicted PGA_v values lower and higher than their recorded values, respectively. Moreover, PGA_v-3 with a lower LLH outperformed the selected attenuation relationships. The lowest LLH was obtained for PGA_v-1. The attenuation relationships are ranked in Table 8 based on different assessment criteria. According to Table 8 and all assessment criteria, it could be concluded that the proposed attenuation relationships in this article outperform other attenuation relationships.

Table 7
The values of error evaluation criteria for PGA_v estimation relations

Models	MAPE%	RMSE	ME	R^2	$R^2_{Adjusted}$	LLH
*PGA_v-1(Present Study)	79.843	0.22	0.012	0.593	0.586	0.049
**PGA_v-3(Present Study)	42.682	0.316	0.081	0.999	0.991	0.386
SZ-17	41.623	0.365	0.073	0.152	0.136	0.612
SP-17	50.670	0.425	0.117	0.039	0.013	0.815
N-5	55.441	0.342	0.069	0.209	0.202	0.500
Z-9	66.267	0.376	0.108	-0.024	-0.043	0.740
G-7	103.569	0.639	0.078	0.179	0.138	1.400

*The proposed model based on the shear wave velocity and objective function of RMSE for PGA_v
**The proposed model based on the fault type and hybrid objective function of MAPE and RMSE for PGA_v

Table 8
Ranking of PGA_v estimation models.

Models	MAPE%	RMSE	ME	R^2	$R^2_{Adjusted}$	LLH
*PGA_v-1(Present Study)	6	1	1	2	2	1
**PGA_v-3(Present Study)	2	2	5	1	1	2
SZ-17	1	4	3	5	5	4
SP-17	3	6	7	6	6	6
N-5	4	3	2	3	3	3
Z-9	5	5	6	7	7	5
G-7	7	7	4	4	4	7

*The proposed model based on the shear wave velocity and objective function of RMSE for PGA_v
**The proposed model based on the fault type and hybrid objective function of MAPE and RMSE for PGA_v

For further investigation and a better comparison of the proposed attenuation relationships with other attenuation relationships, the observed and estimated PGA_v values are presented in Figure 3. As seen, there is greater compliance between the accelerogram and calculated data for the PGA_v-3 model.

For further assessment of the attenuation models to each other, they were investigated and compared in terms of accuracy and standard deviation of residuals in relation to the moment magnitude (M_W). The results are presented in Table 9 where P_a and P_b, respectively, represent the p-values of the slope and y-intercept. The null hypothesis is rejected when the p-values are lower than or equal to the significance level of 5%. A p-value greater than 5% leads to confirmation of the null hypothesis. When the p-values approach 1, the resulting attenuation model with a lower standard deviation will be capable to predict PGA with the higher accuracy.

Table 9
Deviation of residuals versus moment magnitude for PGA_v estimation models.

Models	$(P_a)_{Mw\ vs\ residual}$ *	$(P_b)_{Mw\ vs\ residual}$ **
PGA_v-1(Present Study)	0.354	0.410
PGA_v-3(Present Study)	0.743	0.385
SZ-17	0.575	0.957
SP-17	0.519	0.244
N-5	0.162	0.068
Z-9	0.894	0.422
G-7	0.258	0.224

*The P-value of fitted line slope on the residuals (distribution of models residuals versus M_w)
**The P-value of fitted line intercept on the residuals (distribution of models residuals versus M_w)

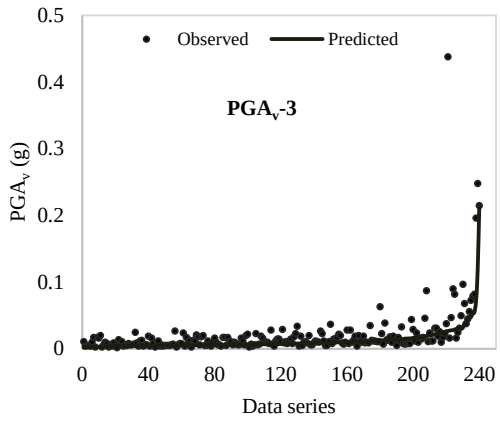

(a) The attenuation relation proposed in present study

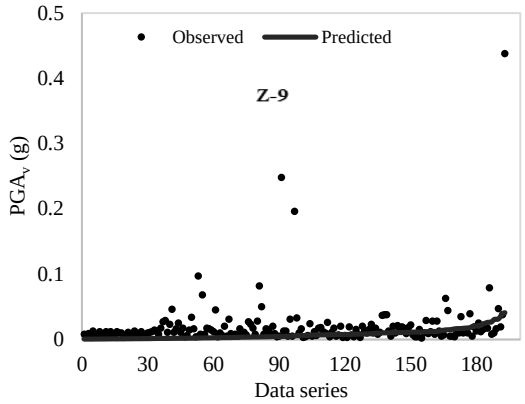

(b) The attenuation relation proposed by Zaré (1999) [11]

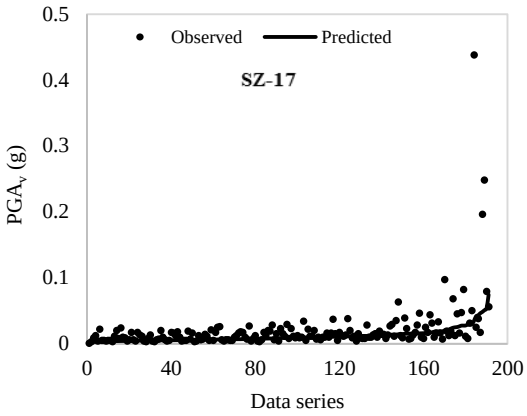

(c) The attenuation relation proposed by Soghrat and Ziyaeifar (2017) [4]

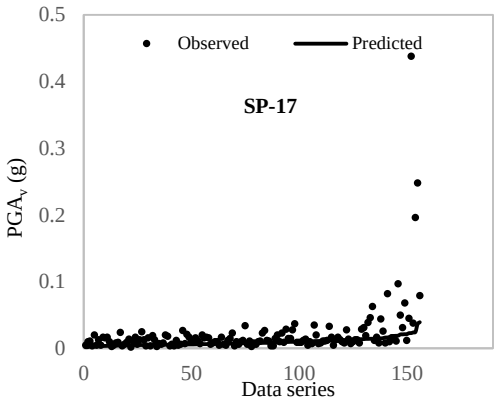

(d) The attenuation relation proposed by Sedaghati and Pezeshk (2017) [13]

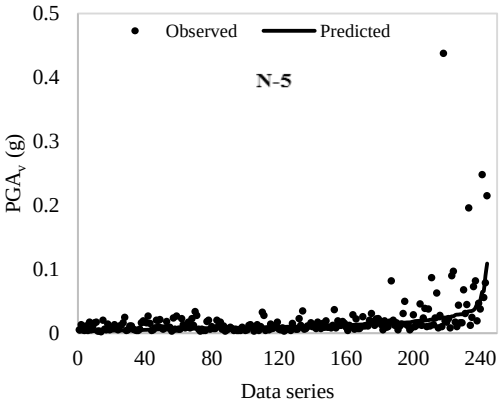

(e) The attenuation relation proposed by Nowroozi (2005) [35]

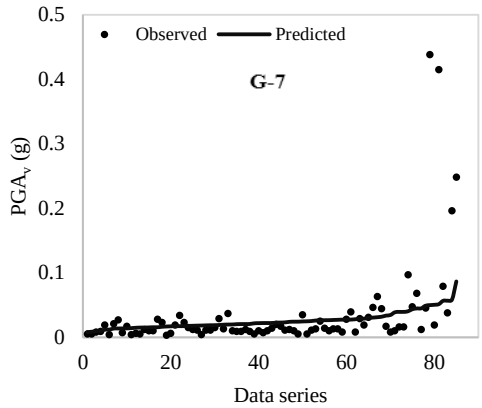

(f) The attenuation relation proposed by Ghodrati Amiri et al. (2007) [36]

Fig. 3. The comparison of the attenuation relationships for estimating PGA$_v$.

According to Table 9, Z-9 followed by PGA_v-3 has the lowest standard deviation due to a high P-value. However, as shown in Table 7, PGA_v-3 has a significantly lower ME than Z-9 and thus is superior to Z-9. Figure 4 shows the line fitted on the residuals versus the moment magnitude for the best and worst PGA_v estimation attenuation models.

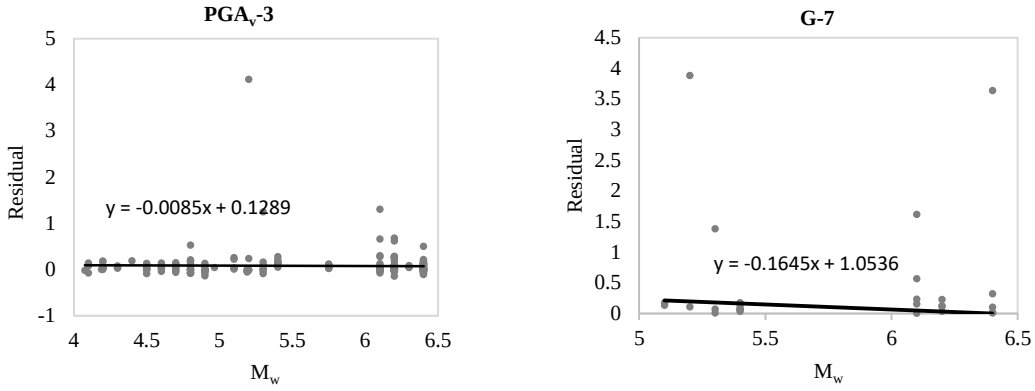

a) The best attenuation relation b) The worst attenuation relation

Fig. 4. Residual distribution versus M_w for the best and the worst PGA_v estimation relations.

Considering MW=6 and Vs30=500 m/s, the PGA_v was estimated for different epicentral distances using different attenuation relationships (Figure 5). The PGAv-3 output has the maximum consistency with the SZ-17 and N-5 output in the vertical direction. There is a small gap between the SP-17 diagram and other mentioned diagrams (the type of distance in this relation is different from the other relations). The G-7 due to the lack of accelerograph data is very different from other charts.

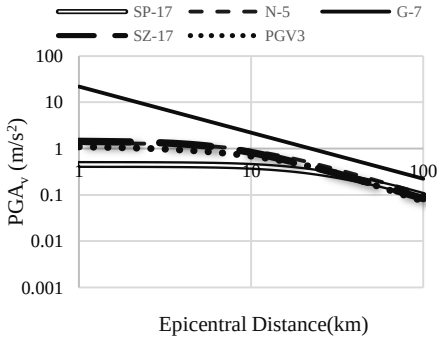

Fig. 5. A comparison between the attenuation models for the horizontal and vertical directions considering M_w=6, V_{s30}=500 m/s (SC=II) for vertical direction.

5. Conclusion

In this study, regarding the importance of the vertical component of PGA in the extent of damage to buildings, PGA estimation in the vertical direction was considered. About 240 earthquake data were gathered from the BHRC with a moment magnitude of 4.1 to 6.4 and the epicentral distance of less than 400 km. Then, using the PSO algorithm, new attenuation relationships were developed for seismic regions in the northern plateau area of Iran. Using different evaluation criteria and the LLH test, the proposed attenuation relationships were compared with those

presented in the literature for the north plateau of Iran, Europe and the Middle East. The obtained results are summarized in following:

- PSO algorithm can be used as a powerful optimization method to improve the accuracy of attenuation relationships.
- The hybrid objective function considered in this study is very effective in improving the accuracy and efficiency of the proposed attenuation models.
- In contrast to the previous attenuation relationships presented by other researchers, some attenuation relationships proposed in this study do not need the shear wave velocity data for the estimation of ground motion acceleration. This characteristic facilitates their application in regions where the shear wave velocity data is not available.
- The attenuation models proposed in this paper outperformed other attenuation relationships in terms of different evaluation criteria and they were relatively highly accurate in the estimation of the PGA.
- The model proposed for estimating PGA_v with the combined objective functions and based on the classification of fault types was highly consistent with the model presented by Soghrat and Ziyaeifar (2017).

Funding

This research received no external funding.

Conflicts of interest

The authors declare no conflict of interest.

References

[1] Moavi M, Adeli M. Investigating the effect of spectral attenuation relationships on the results of seismic hazard probabilistic analysis. Proc. 7th Natl. Civ. Eng. Congr. Sistan Baluchestan Univ. Zahedan, Iran, 7-8 May (In Persian), 2012.

[2] Hajimohammadi B, Zafarani H, Ghalandarzadeh A. Time-Dependent Probabilistic Seismic Hazard Analysis Using the Simulated Records, the Case of Tehran (In Persian). J Struct Constr Eng 2015;1:50–60.

[3] N. PM, Limin H, Michael C. Vertical Seismic Forces on Elevated Concrete Slabs . Pract Period Struct Des Constr 1996;1:88–90. https://doi.org/10.1061/(ASCE)1084-0680(1996)1:3(88).

[4] Soghrat MR, Ziyaeifar M. Ground motion prediction equations for horizontal and vertical components of acceleration in Northern Iran. J Seismol 2017;21:99–125. https://doi.org/10.1007/s10950-016-9586-4.

[5] Terzić A, Pezo L, Mijatović N, Stojanović J, Kragović M, Miličić L, et al. The effect of alternations in mineral additives (zeolite, bentonite, fly ash) on physico-chemical behavior of Portland cement based binders. Constr Build Mater 2018;180:199–210. https://doi.org/10.1016/j.conbuildmat.2018.06.007.

[6] Rahai A, Arezoumandi M. Effect of vertical motion of earthquake on RC bridge pier. 14th World Conf. Earthq. Eng. Seism. Perform. Eval. a Reinf. Concr. Arch Bridg., 2008.

[7] Kallioras S, Graziotti F, Penna A, Magenes G. Effects of vertical ground motions on the dynamic response of URM structures: Comparative shake-table tests. Earthq Eng Struct Dyn 2022;51:347–68. https://doi.org/10.1002/eqe.3569.

[8] Valdés-Vázquez J-G, García-Soto AD, Jaimes MÁ. Impact of the Vertical Component of Earthquake Ground Motion in the Performance Level of Steel Buildings. Appl Sci 2021;11. https://doi.org/10.3390/app11041925.

[9] Ghobarah A. Response of RC structures to near-fault records. Proc. 13th Word Conf. Earthq. Eng. Vancouver, B.C, Canada, 1-6 August, 2004.

[10] Benbouras MA, Kettab RM, Zedira H, Debiche F, Zaidi N. Comparing nonlinear regression analysis and artificial neural networks to predict geotechnical parameters from standard penetration test. Urban Arhit Constr 2018;9:275–88.

[11] Zaré M. Contribution à l'étude des mouvements forts en Iran: du catalogue aux lois d'atténuation 1999.

[12] Ambraseys NN, Douglas J, Sarma SK, Smit PM. Equations for the Estimation of Strong Ground Motions from Shallow Crustal Earthquakes Using Data from Europe and the Middle East: Horizontal Peak Ground Acceleration and Spectral Acceleration. Bull Earthq Eng 2005;3:1–53. https://doi.org/10.1007/s10518-005-0183-0.

[13] Sedaghati F, Pezeshk S. Partially Nonergodic Empirical Ground-Motion Models for Predicting Horizontal and Vertical PGV, PGA, and 5% Damped Linear Acceleration Response Spectra Using Data from the Iranian Plateau. Bull Seismol Soc Am 2017;107:934–48. https://doi.org/10.1785/0120160205.

[14] Ghodrati Amiri G, Razavian Amrei SA, Razavian Amrei SA. Development of PGA Attenuation Relationships for Iran. J Model Eng 2018;16:167–75. https://doi.org/10.22075/jme.2017.4629.

[15] Bagheri A, Amiri GG, Khorasani M, Haghdoust J. Determination of attenuation relationships using an optimization problem. Int J Optim Civ Eng 2011;1:597–607.

[16] Lee C, Ahn J. Flexural Design of Reinforced Concrete Frames by Genetic Algorithm. J Struct Eng 2003;129:762–74. https://doi.org/10.1061/(asce)0733-9445(2003)129:6(762).

[17] Ricardo P, Ronald T. Structural Damage Detection via Modal Data with Genetic Algorithms. J Struct Eng 2006;132:1491–501. https://doi.org/10.1061/(ASCE)0733-9445(2006)132:9(1491).

[18] Shiuly A, Roy N, Sahu RB. Prediction of peak ground acceleration for Himalayan region using artificial neural network and genetic algorithm. Arab J Geosci 2020;13:1–10.

[19] Sobhaninejad G, Noorzad A, Ansari A. Genetic algorithm (GA): A new approach in estimating strong ground motion attenuation relations. Proc. Fourth Int. Conf. Earthq. Geotech. Eng., 2007.

[20] Kennedy J, Eberhart R. Particle swarm optimization. Proc. IEEE Int. Conf. Neural Netw. IV, 1942–1948., vol. 4, IEEE; 1995, p. 1942–8. https://doi.org/10.1109/ICNN.1995.488968.

[21] Poormirzaee R. S-wave velocity profiling from refraction microtremor Rayleigh wave dispersion curves via PSO inversion algorithm. Arab J Geosci 2016;9:673.

[22] Gilani S-O, Sattarvand J, Hajihassani M, Abdullah SS. A stochastic particle swarm based model for long term production planning of open pit mines considering the geological uncertainty. Resour Policy 2020;68:101738. https://doi.org/10.1016/j.resourpol.2020.101738.

[23] Pace F, Santilano A, Godio A. A review of geophysical modeling based on particle swarm optimization. Surv Geophys 2021;42:505–49.

[24] Shafei E, Shirzad A, Rabczuk T. Dynamic stability optimization of laminated composite plates: An isogeometric HSDT formulation and PSO algorithm. Compos Struct 2022;280:114935. https://doi.org/10.1016/j.compstruct.2021.114935.

[25] Poormirzaee R, Moghadam RH, Zarean A. Inversion seismic refraction data using particle swarm optimization: a case study of Tabriz, Iran. Arab J Geosci 2015;8:5981–9.

[26] Poormirzaee R. Comparison of PSO and GA Metaheuristic methods to invert Rayleigh wave dispersion curves for Vs estimation: a case study. J Anal Numer Methods Min Eng 2019;9:77–88.

[27] Izquierdo J, Montalvo I, Pérez-García R, Tavera M. Optimization in water systems: a PSO approach. SpringSim, 2008, p. 239–46.

[28] Khokhar B, Parmar KPS, Dahiya S. An efficient particle swarm optimization with time varying acceleration coefficients to solve economic dispatch problem with valve point loading. Energy and Power 2012;2:74–80.

[29] 2800 Code. 2800 Code, Seismic resistant desing of buildings-Code of the practice of Iran. 4st version (In Persian). n.d.

[30] Code P. Eurocode 8: Design of structures for earthquake resistance-part 1: general rules, seismic actions and rules for buildings. Brussels Eur Comm Stand 2005.

[31] Karimiparidari S, Zaré M, Memarian H, Kijko A. Iranian earthquakes, a uniform catalog with moment magnitudes. J Seismol 2013;17:897–911. https://doi.org/10.1007/s10950-013-9360-9.

[32] Mirzaei N, Mengtan G, Yuntai C. Seismic source regionalization for seismic zoning of Iran: major seismotectonic provinces. J Earthq Predict Res 1998;7:465–95.

[33] Scherbaum F, Cotton F, Smit P. On the Use of Response Spectral-Reference Data for the Selection and Ranking of Ground-Motion Models for Seismic-Hazard Analysis in Regions of Moderate Seismicity: The Case of Rock Motion. Bull Seismol Soc Am 2004;94:2164–85. https://doi.org/10.1785/0120030147.

[34] Delavaud E, Scherbaum F, Kuehn N, Riggelsen C. Information-Theoretic Selection of Ground-Motion Prediction Equations for Seismic Hazard Analysis: An Applicability Study Using Californian Data. Bull Seismol Soc Am 2009;99:3248–63. https://doi.org/10.1785/0120090055.

[35] Nowroozi AA. Attenuation Relations for Peak Horizontal and Vertical Accelerations of Earthquake Ground Motion in Iran: A Preliminary Analysis. J Seismol Earthq Eng 2005;7:109–28.

[36] Ghodrati Amiri G, Mahdavian A, Dana FM. Attenuation relationships for Iran. J Earthq Eng 2007;11:469–92. https://doi.org/10.1080/13632460601034049.